IMAGING OF CONCRETE DEFECTS USING ELASTIC WAVE TESTS

混凝土缺陷影像法

劉 佩 玲** 葉 柏 涼* 游 志 源*
Pei-Ling Liu Bor-Liang Yeh Chih-Yuan Yiu
**教授 *碩士班研究生
國立台灣大學應用力學研究所
**Professor *Graduate student
Institute of Applied Mechanics, National Taiwan University, Taipei, Taiwan 10617, R.O.C.
Institute of Applied Mechanics, National Taiwan University, Taipei, Taiwan 10617, R.O.C.

摘 要

彈性波法是用來評估混凝土品質的一種相當有效的非破壞檢測法。在彈性波試驗中，利用鋼珠或鐵槌敲擊混凝土表面，以產生應力波源，並以感測器測量混凝土表面反應。由於應力波在混凝土內部傳遞時，遇到缺陷會產生反射、折射或繞射行為，故傳回表面之訊號含有內部缺陷資訊。表面訊號經過適當處理後，便可顯現缺陷之位置或尺寸。本文介紹數種利用彈性波建構混凝土缺陷影像的技術，包括表面裂縫影像法、表面裂縫三維掃描法，以及時間域和頻率域的內部缺陷影像法。所建構的影像可用以決定表面裂縫的走向及深度、內部缺陷位置、鋼筋位置，及保護層厚度。文中並以數值算例、模型試驗及現場試驗驗證各種影像法之有效性。

關鍵詞： 混凝土、裂縫、缺陷、彈性波、影像法。

Abstract

The elastic wave test is an effective method for the nondestructive evaluation of concrete structures. In the test, an impact is applied on the surface of the concrete structure, and the response of the concrete due to the impact is measured and recorded. Since the surface response contains information regarding the defect of concrete, the data can be processed to depict the location and size of the defect. This paper presents the principles of various techniques to construct the image of defects in concrete structures using the elastic wave test. The techniques introduced include the imaging of surface-opening cracks, the three dimensional scan of surface-opening cracks, and the imaging of internal defects using time domain or frequency domain signals. The images can be used to determine the location of a surface-opening crack, an internal defect, reinforcing steel bars, or the covering thickness. Numerical examples, model tests, and in-situ tests are presented to verify the effectiveness of these methods.

Keywords: concrete, crack, defect, elastic waves, imaging.

1. INTRODUCTION

Reinforced concrete is the most commonly used construction material nowadays. Since the tensile strength of concrete is only about 10% of its compressive strength, cracks often develop in concrete. In addition to cracks, voids and honeycombs may also present in the interior of concrete. The existence of such flaws may decrease the strength of the structure, and failure of the structure may follow. Therefore, the detection of defects in reinforced concrete is indispensable in the safety assessment of reinforced concrete structures.

Recently, stress waves have been widely used to detect flaws in concrete. Sakata and Ohtsu [1] applied ultrasonic spectroscopy to evaluate vertical cracks. Chang and Wang [2] used ultrasonic waves to scan surface opening cracks. In addition to ultrasonic waves, many researchers have adopted transient elastic wave tests in the detection of cracks in concrete. Lin and Sansalone [3] used the impact echo method to detect flaws in concrete beams and columns. Wu *et al.* [4] developed an inverse method to detect the depth of vertical cracks based on phase information. Lin and Su [5] and Lin *et al.* [6] applied the impact echo method to measure the depth of cracks in reinforced concrete. Liu *et al.* [7] proposed a migration imaging method that can depict the location of a surface-opening crack on a test section. The migration method was extended to construct the 3D image of the crack [8]. Kuo *et al.* [9] applied optimization techniques to locate the crack tip. Ohtsu and Watanabe [10] developed the stack imaging method for flaw detection.

In this paper, various methods for constructing images of the surface-opening cracks and interior defects of concrete structures are presented. The elastic wave tests are adopted in these methods. Either time-domain or frequency-domain data are processed to display the image. The images can be used to determine the location of a surface-opening crack, an internal defect, reinforcing steel bars, and the covering thickness of the rebars.

2. ELASTIC WAVE TEST

In the elastic wave test, a vertical point source is applied by dropping a steel ball on the surface of a concrete structure. Stress waves are generated and propagated in the concrete structure. If the waves encounter an interface or inhomogeneity, they will be reflected, refracted, or diffracted. Then, a transducer is used to measure the response on the concrete surface. The received voltage signals are fitted in a preamplifier and recorded by a digital oscilloscope or a notebook computer for subsequent data processing.

The time function of the impact was very close to a half sine function, the duration of which is dependent on the size of the ball. The larger the ball is the longer the source duration is. In real applications, the source duration is usually greater than 50μsec. Hence, the dominant frequency is less then 20kHz. Since the longitudinal wave velocity of concrete is about 3,000 ~ 5,000m/sec, the wavelength of the induced longitudinal wave is greater than 150mm, which is much larger than the maximum size of the aggregate. Therefore, concrete can be considered a homogeneous material.

3. IMAGING OF SURFACE-OPENING CRACKS

The elastic wave test has its parallel in seismic exploration. In the seismic test, a source is also applied on the surface of the earth. Then, the surface response of the earth is received by an array of geophones. Finally, the signals are processed to produce an image of the geological structure.

The procedure of signal processing in reflection seismology mainly includes the following steps: static and dynamic corrections, horizontal stacking, migration, and velocity analysis [11]. Because there are fundamental differences between a cracked concrete structure and the earth structure, most of these steps are either unsuitable or unnecessary in crack detection except migration. For example, the earth usually has a layered structure and the dip angles of the layers are usually small. A concrete block, on the other hand, is homogeneous from a macroscopic point of view. There is no layer interfaces in the concrete, but cracks may exist, and the cracks usually have high dip angles.

Migration can compress diffraction signals back to their originating point and depict the location of the diffraction point. The tip of a crack is certainly a diffraction point. Therefore, the idea of migration can be adopted to locate the tip of a surface-opening crack in the concrete.

When a source is applied on the surface of a concrete structure, elastic waves are generated and propagated in the structure. Waves reaching the crack will be reflected, and the waves reaching the crack tip will be diffracted and arrive at the other side of the crack. In addition, surface waves will be generated. The amplitude of the surface wave is much larger than that of the body wave. If the source and receiver are on the same side of the crack opening, the surface response is dominated by the surface wave. Unfortunately, surface waves do not contain any useful information about the crack. Therefore, the source and receiver should be placed on the opposite sides of the crack opening. In that case, the signals received are mostly diffracted waves because the surface waves are blocked by the crack.

The principle of migration is as follows: Consider a signal that is emitted from the source, diffracted at a point, and arrives at the receiver. Suppose the travel is v. Then, the travel distance of the signal is vt. If the diffraction path is unknown, any point in the medium with the same travel distance is a possible diffraction point. Therefore, the diffraction point should fall on an ellipse with the source and receiver as its foci, as shown in Fig. 1. If two ellipses are drawn using different diffracted signals, the diffracted point must be located at the intersection of the two ellipses.

A migration image can be constructed following this idea. We firstly draw a blank half-plane. Then, an ellipse is constructed for each of the data points in

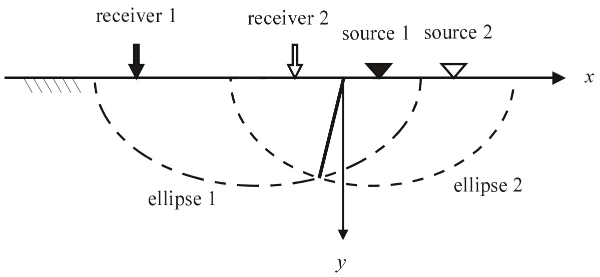

Fig. 1 Principles of migration

the response curve according to the travel distance.Since the amplitude of the data points varies, the elliptic trajectories are of different magnitudes. Representing the magnitude by grayscale, we get a grayscale image. Since there is a visible change in the response curve when the first diffracted signal arrives, the ellipse of the first diffraction can be located on the image. If more than one response curve are migrated, the crack tip is simply located at the common intersection of the ellipses of the first arrivals.

The grayscale image obtained by migration can only depict the location of the crack tip, not the crack itself. To make the image more easily read, a line segment is superposed to the grayscale image to represent the crack. The crack tip is located at the intersection of the first-arrival ellipses. Therefore, to draw the line segment, the travel times of the first arrivals are determined first. Then, simultaneous equations are solved to find the intersection of the ellipses. Once the crack tip is found, a line is drawn connecting the crack opening and crack tip.

Two model tests were conducted to illustrate the migration method. The experiments were conducted on two concrete models. The first model has a vertical slit, the width and depth of which are 2.5mm and 90mm, respectively. The second model has a 45° slit, the width and length of which are 1.5mm and 120mm, respectively.

Figures 2 and 3 show the migration images of the concrete models. The × symbol in the image denotes the actual location of the crack tip. It is seen in both image that the crack is surrounded by a zero-grayscale zone, corresponding to quiescent part of the curve before the first diffraction arrives. Outside the zero-grayscale zone, there is a bright zone, corresponding to the positive signals of the displacement curve. Theoretically, the crack tip is located at the sharp corner of the zero-grayscale zone. The crack is also represented by a solid line. It is seen that the crack tip obtained by the intersection of the first-arrival ellipses is very close to the actual tip location in both cases. These model tests verify that the proposed imaging method can display real cracks successfully.

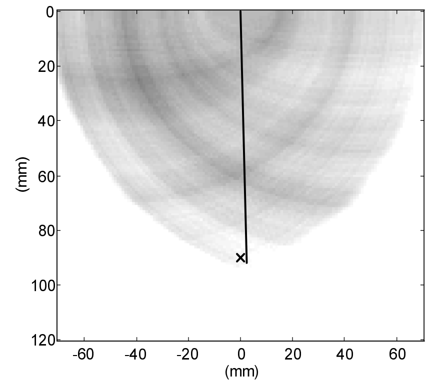

Fig. 2 Migration image of a vertical crack

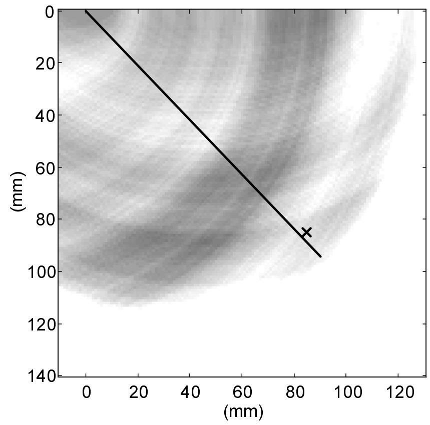

Fig. 3 Migration image of a 45° crack

4. SCAN OF SURFACE-OPENING CRACKS IN REINFORCED CONCRETE

The method introduced in the preceding section yields a two dimensional image of a surface-opening crack in a concrete structure. The migration method can be extended to construct the 3D image of the crack. Similar to the 2D migration method, two elastic wave tests are performed on the concrete structure with the source and receiver placed on the opposite sides of the crack opening. If ellipses are drawn using the first arrivals of these tests, the diffraction point must be located at the intersection of the two ellipses. Connecting the crack opening and the intersection, one obtains an image of the crack on the test section. Move the source and receiver along the crack opening to a new test section, and perform the test again. One can obtain a crack image of the new section. Repeating the procedure several times, one obtains a sequence of crack images. A 3D image of the crack can be constructed simply by connecting all the 2D crack images in a 3D draw.

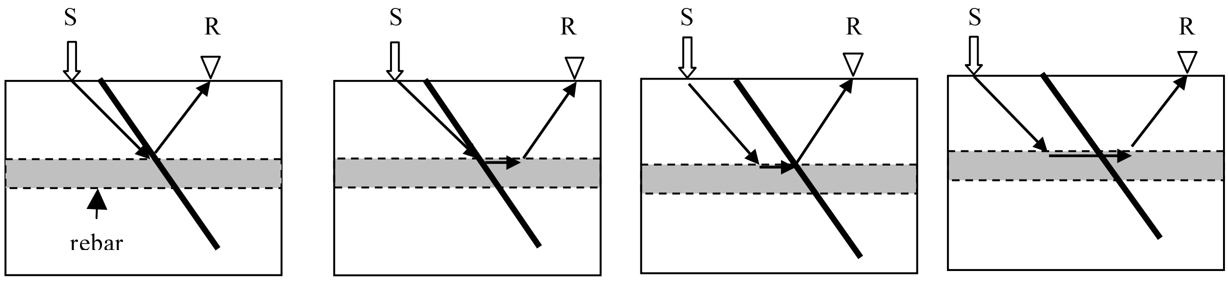

Fig. 4 Possible paths of the first arrival from the rebar

This method can produce the image of a surface-opening crack in pure concrete successfully. However, when there is reinforcement in the concrete, the signals are influenced by the reinforcing bars. Longitudinal waves propagate much faster in steel bars than in concrete. Therefore, the first arrival does not necessarily come from the crack tip.

Except diffracting from the crack tip, there are four other possible propagating paths for the first arrival, as shown in Fig. 4. One can show that the travel time of the refracted signal is always shorter than that of the direct wave. However, refraction occurs only when the horizontal distance between the source and the receiver is far enough. Therefore, which path the first arrival takes depends on the geometry of the test layout.

If the first arrival comes from the rebar, it contains no information about the crack tip. In that case, the intersection of the ellipses no longer indicates the location of the crack tip. One can show that when the source and receiver are placed directly above the rebar, the crack length can be detected correctly only when the crack length is shorter than the covering thickness. The detectable length increases as the test section departs from the rebar. Therefore, the influence of the rebar is maximal when the source and receiver are right above the rebar. The influence decreases as the test section is moved away from the rebar. Accordingly, the scan image of the crack may be distorted near the rebar, and the distortion diminishes as the test section leaves the rebar. Although the image may be distorted, it still provides useful information.

Figure 5 shows the numerical results of scanning a reinforced concrete block with an 8cm vertical crack. Two different reinforcement conditions are considered: (a) No rebar exists. (b) There is a rebar perpendicular to the crack. The diameter of the rebar is 2cm and the covering thickness is 4cm. The longitudinal wave velocities of the concrete and rebar are 4160m/s and 5920m/s, respectively. The source is located at 2cm and 6cm to the left of the crack opening in the first and second test, respectively. The receiver is located at 8cm and 4cm to the right of the crack opening in the first and second test, respectively. All test sections are perpendicular to the crack opening, and the distance between successive test sections is 1cm.

When there is no rebar, a correct image of the crack is obtained, as expected. When the rebar is present, the crack edge becomes concave. Furthermore, the crack image warps and is no longer a vertical plane.

It is seen in Fig. 6(b) that the depth of the crack image at $y = 0$ is 3.5cm, which is shortest along the

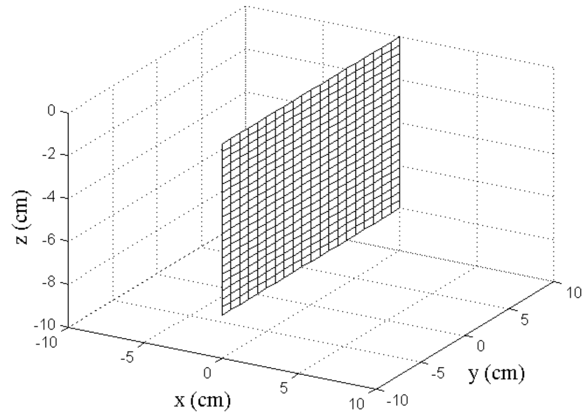

(a) no rebar

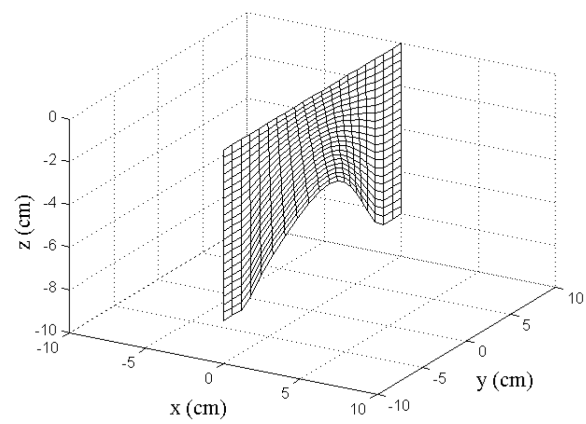

(b) a rebar with 4cm covering

Fig. 5 Scan image of the vertical crack

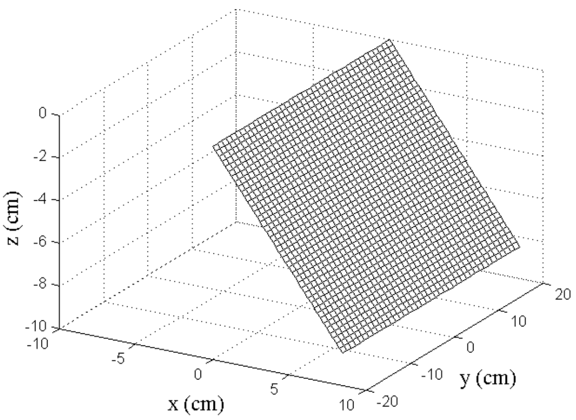

(a) no rebar

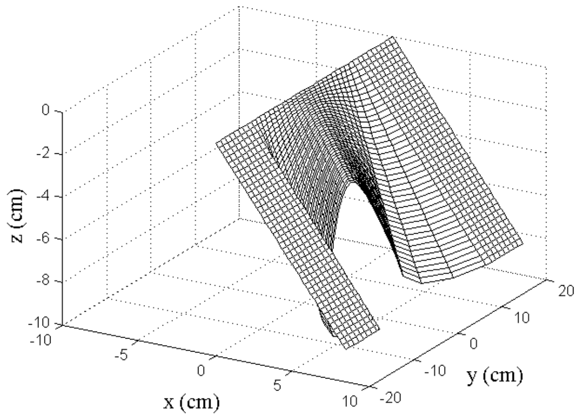

(b) a rebar with 4cm covering

Fig. 6 Scan image of the 45° crack

crack. This indicates that the rebar is located at $y = 0$ with a covering somewhat thicker than 3.5cm. Obviously, one can estimate the covering thickness of the rebar using the crack image.

The ability of the method to scan a real crack was examined by a model test. The experiments were conducted on a concrete model with an embedded rebar. The model had a vertical slit with a constant depth of 12cm. The covering thickness and diameter of the rebar are 4cm and 2cm, respectively. The longitudinal wave velocities of concrete and rebars were 4160m/s and 5863m/s, respectively.

The scan image of the crack around the rebar is shown in Fig. 7. As expected, the crack edge is concave around the rebar. The crack length is approximately equal to the covering thickness 4cm right above the rebar. The crack length increases as the test section is moved away from the rebar. Finally, the image restores its correct length when the test section is about 13cm away from the rebar.

Similar to the numerical examples, the location and the covering thickness of the rebar can be determined by

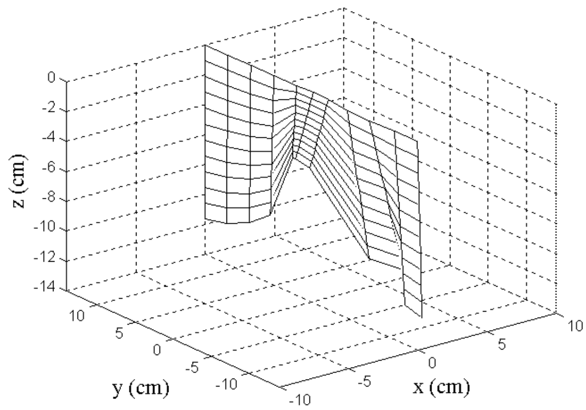

Fig. 7 Scan image of the model crack

the depth of the crack edge at $y = 0$, which is approximately 4cm.

5. IMAGING OF INTERNAL DEFECTS USING TIME DOMAIN SIGNALS

It is mentioned that the surface waves cannot propagate across a surface-opening crack. Therefore, if the source and receiver are placed on the opposite sides of the crack opening, the received signal does not contain surface waves. This is advantageous because surface waves do not contain any information about the defect. Furthermore, the useful reflected or diffracted waves will not be submerged in the surface wave.

Unfortunately, the surface wave is unavoidable in the case of internal defects. Therefore, it is very difficult to construct a migration image using merely two records. One possible way of detecting an internal defect is to perform a series of tests along a line. Then, draw the response curves side by side. If there are no internal defects, the curves should look alike. On the other hand, if distortion is observed in some curves, there should be some inhomogeneity under those test points.

For example, consider a concrete block with a horizontal crack 15cm under the surface. Fifteen numerical simulations are performed to compute the surface displacements of the block. The source and receiver are 5cm apart in each simulation. The distance between any two successive sources is 4cm. The source locations of the 8th to the 12th tests are right above the crack.

Figure 8 shows the 15 response curves of the concrete block. It is seen that for curves 1 to 4, and curves 13 to 15, there is basically no signal after the

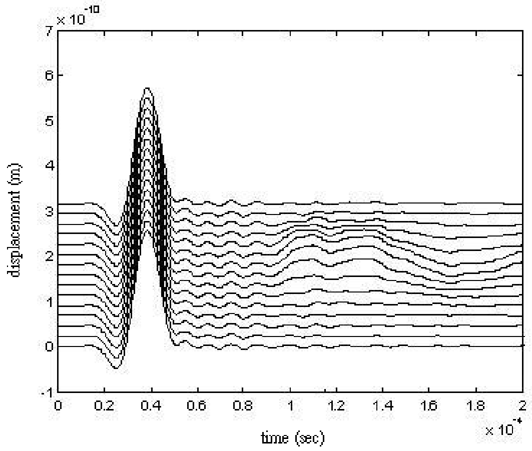

Fig. 8 Consecutive displacement curves

Rayleigh wave passes. The shapes of curves 5 to 12 look quite different. Large fluctuations are observed after the Rayleigh wave in these curves, and the fluctuation of curves 8 and 9 is the largest among them. Apparently, there is a defect under these test points. However, it is difficult to judge how deep and what shape the defect is from these curves.

To overcome the difficulties, the migration imaging method can be adopted here. Figure 9 shows a series of migration images of the model. The solid line segments represent the internal crack. Each image is constructed following the same procedure as in the imaging of surface-opening crack, and three consecutive traces are used for each image. For all the images, there is a black semi-ellipse surrounded by a bright zone under the source and receiver. That is from the Rayleigh wave. If the source and receiver are not placed right above the crack, there are only blurry ripples outside the bright zone. Theoretically, this zone should be of zero grayscale because there is no signal. However, ripples always exist because of noise. As the source and receiver are moved toward the crack, another bright band shows up. The closer the source and receiver are to the crack, the brighter and wider the band is. The inner rim of the band also reveals the depth of the crack. Obviously, one can determine where the crack is by comparing these images.

Although one can detect the location of an internal defect using the above successive images, this method does not provide a direct picture of the defect. There is still need for improvement.

Notice that the influence of the crack is the strongest when the source and receiver are right above the crack. Therefore, we take a slice of image directly under the source and receiver from each of the successive images. Then, assemble the slices according to their original order. Figure 10 shows the assembled image of the crack. There is a bright zone on top of the image. This is from the Rayleigh wave. There is another bright zone on the image. Compared with the true crack location, the zone reveals the width and depth of the crack. Apparently, the image yields direct information on where and how large the defect is.

One should notice that the thickness of the bright zone is not equal to the thickness of the defect. This is because almost all energy is reflected when a wave encounters a crack. No wave is reflected from the bottom of the crack. Therefore, it is impossible to construct an image showing the bottom of the crack. One should also know that the bright zone is somewhat wider than the crack. This is because there are still reflected or diffracted signals even when the source and

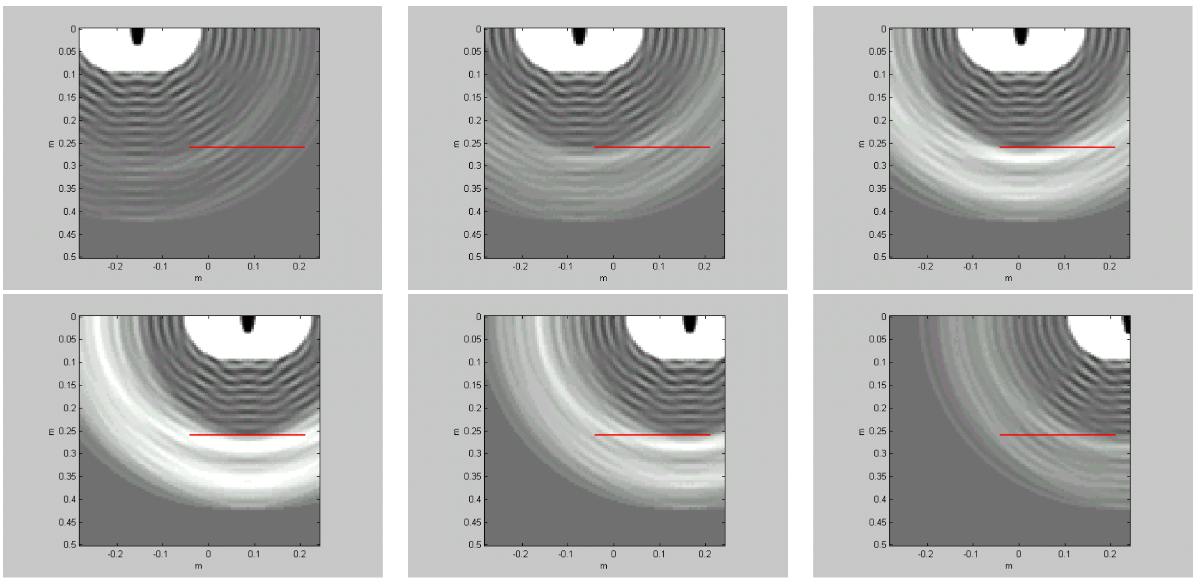

Fig. 9 A series of migration images of an internal horizontal crack

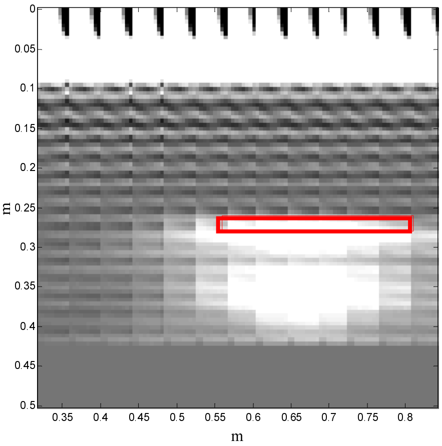

Fig. 10 Assembled image of an internal horizontal crack

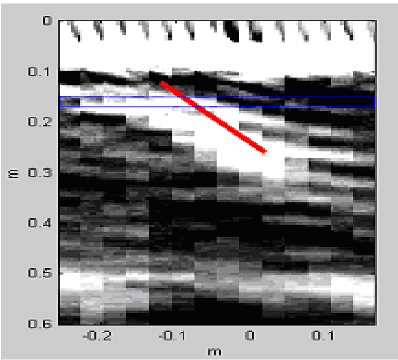

Fig. 11 Assembled image of the 45° model crack

receiver are not above the crack. This should be acceptable because the estimation is on the safe side.

Figure 11 shows the assembled image obtained in a model test. The concrete model has a 45° slit. Similar to the numerical results, there is a Rayleigh bright zone. The 45° crack is also depicted in the image. In addition to these bright zones, there is a horizontal bright band located at the bottom of the image. Since the thickness of the model is 50cm, this band apparently denotes the bottom of the model. Although the test image is not as clear as the numerical image, the defect can be detected without difficulty.

6. IMAGING OF INTERNAL DEFECTS USING FREQUENCY DOMAIN SIGNALS

The impact echo method [3] is a well established NDT method on concrete structures. In this method, elastic wave tests are also performed on the concrete. Then, the recorded time signals are transformed into the frequency domain using the fast Fourier transform. If there is an internal crack or void, one should find a peak in the spectrum. The frequency of the peak f_d can be related to the depth of the defect, D, by the following formula:

$$D = \frac{C_p}{2f_d} \tag{1}$$

where C_p is the velocity of longitudinal waves of the concrete.

The impact echo method is very effective when it is applied to plain concrete. However, if the concrete is heavily reinforced, the spectrum becomes very complicated. In that case, it is difficult to detect an internal defect by examining a single spectrum. One possible solution is to put the spectra of several tests together. Then, try to compare the pattern of these spectra to see if any spectrum deviates from the regular pattern.

If the test area is large and there are hundreds or thousands of test points, such comparison is time consuming. In order to speed up the process, one may construct a "B-scan" image using the impact echo data. To do this, one has to select a test line on the concrete surface and perform impact echo tests along that line. After completing the tests, represent the spectral amplitude by color scale:

$$c = \begin{cases} 255 & a > a_{\max} \\ 255\ \dfrac{a - a_{\min}}{a_{\max} - a_{\min}} & a_{\min} < a < a_{\max} \\ 0 & a < a_{\min} \end{cases} \tag{2}$$

where a is the amplitude of the spectrum, $a_{\max}$ and $a_{\min}$ are the upper and lower bounds of the amplitude, and c is the corresponding color scale. If a exceeds $a_{\max}$, the color scale is set to 255. If a is less than $a_{\min}$, the color scale is set to 0. One can use $a_{\max}$ and $a_{\min}$ to adjust the contrast of the image. Finally, construct a 2D image using the test position as the horizontal axis and the frequency as the vertical axis.

The spectral B-scan image yields the defect information on the vertical section under the test line. Theoretically, if there is no defect on the test section, the 2D image should contain only horizontal stripes. No color variation should be observed along the horizontal direction. On the other hand, if some irregularities exist, there may be a defect. As an example, Fig. 12 shows the spectral B-scan image of a concrete model. It is seen that there is a red-yellow band in the frequency range 400 ~ 900Hz. This is due to the resonance of the receiver. For test positions 1 ~ 3 and 9 ~ 11, there is also a red band near 4.2kHz. Since the longitudinal velocity C_P = 4267m/s, and the thickness

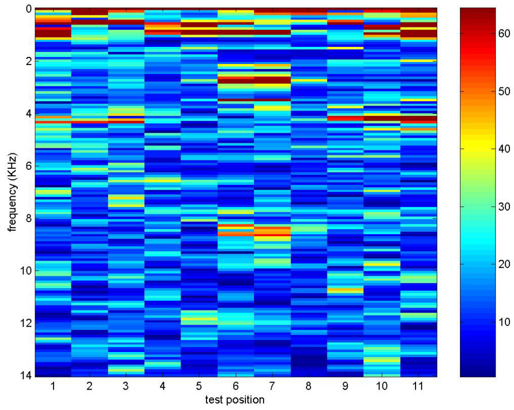

Fig. 12 Spectral B-scan image of the horizontal model crack

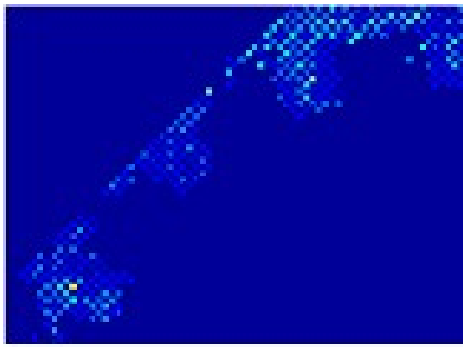

Fig. 13 Spectral C-scan image of a concrete plate

of the model is 50cm. This peak corresponds to the bottom of the concrete block. For test positions 6 ~ 8, the peak frequency is shifted to about 3kHz. This indicates that there is an internal defect in this range so that the travel distance between the source and the bottom is increased. As a result, the peak frequency is reduced. One can also find a red zone near 8.5kHz in this range. According to Eq. (1), This peak corresponds to a defect of 25.1cm deep. That is very close to the actual depth, 25cm, of the model crack.

The spectral B-scan image is useful in the detection of internal defect. Nevertheless, the color at each point does not provide any information. One has to check the discontinuity in the horizontal stripes to see if there is a defect. Hence, the image is not a direct depiction of the internal defect.

Another way of presenting the spectral data is to construct an image for a horizontal section. Similar to the ultrasonic C-scan, the impact echo tests are performed on an area on the concrete surface. After completing the tests, perform fast Fourier transform on the data. Then, select the depth of the horizontal section to be inspected, and determine the corresponding frequency using Eq. (1). For each point in the test area, represent the spectral amplitude by color scale. Finally, construct a spectral image for the horizontal section.

Theoretically, the color of the whole section should be homogeneous if no defect exists. However, if the section does contain a defect, there will be peaks in the spectra. Hence, the color of the defect zone should be different. One can determine if there is a defect simply by examining the color variation of the image. Apparently, the spectral C-scan image is a much better presentation of the defect than the spectral B-scan image, in which the color varies with depth.

Because of concrete inhomogeneity, noise, and numerical errors, the spectrum may fluctuate rapidly. Hence, the color of two neighboring pixels may be quite different even when the test points are above the same horizontal crack. As a result, the spectral C-scan image does not always show a clear picture of the defect. To improve its quality, one can stack the images in a selected frequency range (or depth range) together. This will help smoothing out the image. Alternatively, one can use the maximum color scale of each pixel in the frequency (depth) range to construct the image. Experience shows that the maximum image is much better than the original or stack image.

Figure 13 shows the spectral C-scan image (maximum image) of a concrete plate in a power plant. The inspection depth is 12cm ~ 15cm. It is seen that there may be defects near the upper right corner and lower left corners of the test area. In order to verify the result, cores were taken from the plate near the defect zones. It was found that there are indeed horizontal cracks in these areas. Since the plate is 2.4m thick and is embedded with 7 layers of reinforcing bars, it would be extremely difficult to detect the cracks if other methods were adopted.

7. CONCLUSIONS

This paper introduces the principles of several techniques to construct the image of defects in concrete structures using elastic wave tests. The techniques introduced include the imaging of surface-opening cracks, the three dimensional scan of surface-opening cracks, and the imaging of internal defects using time domain and frequency domain signals.

The images can be used to determine the location of either a surface-opening crack or an internal defect. The 3D image of a surface-opening crack can also be used to determine the location of reinforcing bars and the covering thickness. In addition, it can be used to judge whether the crack penetrates through the reinforcing bars. All these methods are verified by numerical examples, model tests, and in-situ tests.

The imaging methods provide the most direct information on the concrete interior. After proper training, an inspector is able to identify the defect zone of a concrete structure simply by viewing the images. No complicated interpretation is required. Therefore, the imaging methods can serve as useful tools in the nondestructive evaluation of concrete structures. However, to construct an image usually requires lots of response signals. Hence, the test stage is often time consuming. It is hoped that more efficient equipment will be developed soon such that the techniques can be put into practice more extensively in the future.

REFERENCES

[1] Y. Sakata and M. Ohtsu, "Crack evaluation in concrete members based on Ultrasonic Spectroscopy," *ACI Materials Journal*, Vol. 92, No. 6, 1995, pp. 686–698.

[2] Y. F. Chang and C. Y. Wang, "A 3-D image detection method of a surface opening crack in concrete using ultrasonic transducer arrays," *Journal of Nondestructive Evaluation*, Vol. 16 No. 4, 1997, pp. 193–203.

[3] Y. Lin and M. Sansalone, "Detecting flaws in concrete beams and columns using the impact-echo method," *Materials Journal of the American Concrete Institute*, July/August 1992, pp. 394–405.

[4] T.-T. Wu, J. S. Fang and P.-L. Liu, "Detection of the depth of a surface-breaking crack using transient elastic waves," *J. Acoust. Soc. Am.*, Vol. 97, No. 3, 1995, pp. 1678–1686.

[5] Y. Lin and W. C. Su, "The use of stress waves for determining the depth of surface-opening cracks in concrete structures," *ACI Materials Journal*, Vol. 93, No. 5, 1996, pp. 494–505.

[6] Y. Lin, T. Liou and C. Hsiao, "Influences of reinforcing bars on crack depth measurement by stress waves," *ACI Materials Journal*, Vol. 95, No. 4, 1998, pp. 407–418.

[7] P.-L. Liu, C.-D.Tsai and T.-T. Wu, "Imaging of surface-breaking concrete cracks using transient elastic waves," *NDT&E International*, Vol. 29, No.5, 1996, pp. 323–331.

[8] P.-L. Liu, Y.-C. You and T.-T. Wu, "Scan of surface-opening cracks in reinforced concrete using transient elastic waves," *NDT & E International*, Vol. 34, No. 3, 2001, pp. 219–226.

[9] M. K Kuo, T. R. Lin, P.-L. Liu and T.-T. Wu, "Locating the crack-tip of a surface-breaking crack. part I. line crack," *Ultrasonics*, Vol. 36, 1998, pp. 803–811.

[10] O M. htsu and T. Watanabe, "Stack imaging of spectral amplitudes based on impact-echo for flaw detection," *NDT&E International*, Vol. 35, No. 3, 2002, pp. 189–196.

[11] K. H. Waters, *Reflection Seismology*, John Wiley and Sons, New York, 1981.

Pei-Ling Liu (劉 佩 玲) received her B.E. and M.S. degrees in civil engineering from National Taiwan University in 1979 and 1981, respectively, and the Ph.D. degree in civil engineering from the University of California, Berkeley in 1989. She joined the faculty of the Institute of Applied Mechanics, National Taiwan University in 1989. She is now the director and full professor of the Institute. Her major research interests are in safety evaluation of structures, nondestructive testing of structures and reliability analysis.

Bor-Liang Yeh (葉 柏 涼) is a Ph.D. candidate in the Institute of Applied Mechanics, National Taiwan University.

Chih-Yuan Yiu (游 志 源) is a Ph.D. candidate in the Institute of Applied Mechanics, National Taiwan University.

收稿日期 93 年 6 月 1 日、修訂日期 93 年 6 月 10 日、接受日期 93 年 6 月 13 日
Manuscript received June 1, 2004, revised June 10, 2004, accepted June 13, 2004